

ILLUMINATION WAVELENGTH EFFECT ON ELECTRICAL PARAMETERS OF A PARALLEL VERTICAL JUNCTION SILICON SOLAR CELL UNDER STEADY STATE AND UNDER IRRADIATION

Alioune Badara Dieng¹, Boureima Seibou², Seydi Ababacar Ndiaye³, Mamadou Wade⁴, Marcel Sitor Diouf⁵, Ibrahima LY⁶, Grégoire Sissoko⁷

¹Faculty of Science and Technology, University Cheikh Anta Diop, Dakar-Senegal

²Mining School of Niamey-Niger

³Ecole Supérieure polytechnique de Daar-Senegal

⁴Ecole Polytechnique of Thies, EPT, Thies, Senegal

⁵Faculty of Science and Technology, University Cheikh Anta Diop, Dakar-Senegal

⁶Ecole Supérieure polytechnique de Daar-Senegal

⁷Faculty of Science and Technology, University Cheikh Anta Diop, Dakar-Senegal

Abstract

In this article we made a theoretical study of a solar cell in parallel vertical junction under monochromatic illumination in static mode and under irradiation. The resolution of the continuity equation which governs the electron scattering process in the base help us to establish the electrons density expression and deduce expressions of photocurrent density and photovoltage depending on the wavelength λ , recombination velocity at the junction S_f and irradiation parameters. Expressions series resistors and the shunt according to the wavelength, the recombination velocity at the junction and irradiation parameters are obtained from the photovoltage and photocurrent density. We have studied the influence of the variation of the wavelength on the electrons density in the base, the photocurrent, photovoltage and the shunt and series resistors.

Keywords – Silicon Vertical Junction-Wavelength -Irradiation-Shunt and Series Résistances

1. INTRODUCTION

We will make, through this article, a theoretical study of a vertical junction solar cell in parallel monochromatic illumination under static mode and under irradiation. The resolution of the continuity equation help us to establish the expression of the minority charge carriers density in the base and deduct expressions photocurrent density and photovoltage.

The series and shunt resistors were subsequently deducted. We will study in this article the impact of the change in wavelength on all the above listed parameters.

This study we focused on the wavelengths of the visible

2. THEORY

We consider a solar cell type of parallel vertical junction n^+ -p-p whose structure may be represented as follows:

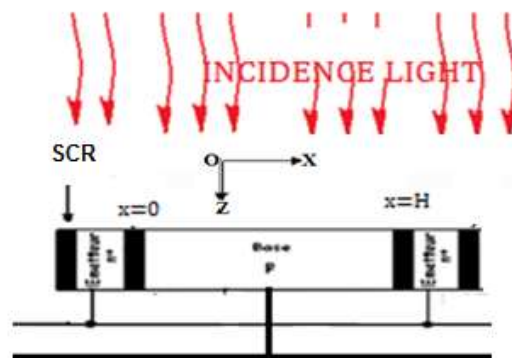


Fig.1: Parallel vertical junctions of a solar cell

When the solar cell is illuminated, there are creation of electron-hole pairs in the base.

The behavior of the minority carriers in the base (electrons) is governed by the continuity equation including all the phenomena which cause the variation of the electrons density according to the width x of the base, its depth z , the recombination velocity to the junction, of the wavelength and irradiation parameters. Solving this equation will enable us to have initially expressing minority carriers density from the base and deduct those quantities and other solar cell's electrical parameters.

The continuity equation in static mode is presented in the form:

$$D \cdot \frac{\partial^2 \delta(x)}{\partial x^2} - \frac{\delta(x)}{\tau} = -G(z) \quad (1)$$

$\delta(x)$ describes the photogenerated minority charge carriers.

. D is the coefficient diffusion. τ is the average lifetime of carriers.

. G (z) is the overall generation rate of minority charge carriers according to the depth z of the base.

The continuity equation can still be written as follows:

$$\frac{\partial^2 \delta(x)}{\partial x^2} - \frac{\delta(x)}{L^2} + \frac{G(z)}{D} = 0 \quad (2)$$

$L(kl, \phi) = \frac{1}{\sqrt{kl \cdot \phi + \frac{1}{L_o^2}}}$ is the diffusion coefficient

[1]. L_o is the diffusion coefficient with the absence of irradiation. Kl and ϕ indicate the coefficient of damage and the radiation energy.

The expression of the overall generation of minority charge carriers rate is of the form:[2]

$$G(z, \lambda) = \alpha_i (1 - R(\lambda)) \cdot F \cdot \exp(-\alpha_i \cdot z) \quad (3)$$

R (λ) is the monochromatic reflection coefficient; F is the incident photon flux from a monochromatic radiation. α is the coefficient of monochromatic reflection.

$$\frac{\partial^2 \delta(x)}{\partial x^2} - \frac{\delta(x)}{L^2} = -\frac{G(z)}{D} \quad (4)$$

2.1 Solution of the Continuity Equation

- Special solution :

$$\delta_1(x) = \frac{L^2}{D} \alpha_i (1 - R(\lambda)) \cdot F \cdot \exp(-\alpha_i \cdot z) \quad (5)$$

-solution of the equation with second member:

$$\delta_2(x) = A \cosh\left(\frac{x}{L}\right) + B \sinh\left(\frac{x}{L}\right) \quad (6)$$

-as the general solution is:

$$\delta(x, z, \lambda, Sf, kl, \phi) = \left[A \cosh\left(\frac{x}{L}\right) + B \sinh\left(\frac{x}{L}\right) + \frac{L^2}{D} \cdot \alpha_i (1 - R(\lambda)) \cdot F \cdot \exp(-\alpha_i \cdot z) \right] \quad (7)$$

2.2 Search the Coefficients A and B

- The boundary conditions:

-as at the junction (x = 0) we have:

$$D \cdot \frac{\partial \delta(x, z, \lambda, kl, \phi)}{\partial x} \Big|_{x=0} = Sf \cdot \delta(x, z, \lambda, kl, \phi) \Big|_{x=0} \quad (8)$$

Sf is the recombination velocity at the junction. This is a phenomenological parameter that describes how the base minority carriers go through the junction. It can be divided into two terms[3].

We have $Sf = Sf_o + Sf_j$

Sf_o induced by the shunt resistance, is the intrinsic recombination velocity. It depends only on the intrinsic parameters of the solar cell.

Sf_j reflects the current flow imposed by an external charge and sets the operating point of the solar cell

-At The middle of the base ($x = \frac{H}{2}$) .The structure of the

solar cell, with two identical junctions on either side of the base, portends equation (9) below:

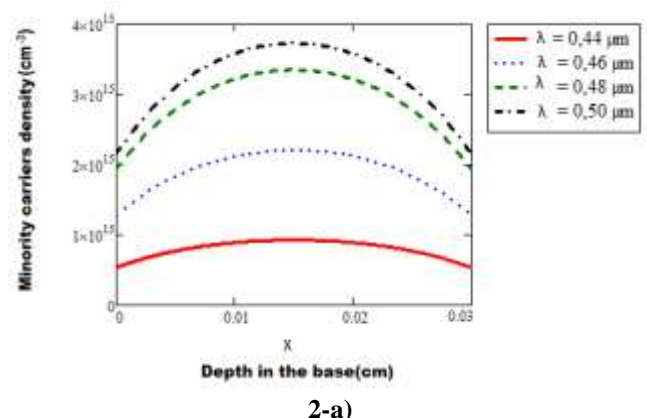
$$D \cdot \frac{\partial \delta(x)}{\partial x} \Big|_{x=H/2} = 0 \quad (9)$$

H is the thickness of the solar cell's base

3. RESULTS AND DISCUSSION

3.1 Density Profile of Minority Carriers in the Base

Fig. 2-a and 2-b show the profile of the density of minority carriers in the base according to its width X there on different values of the wavelength λ



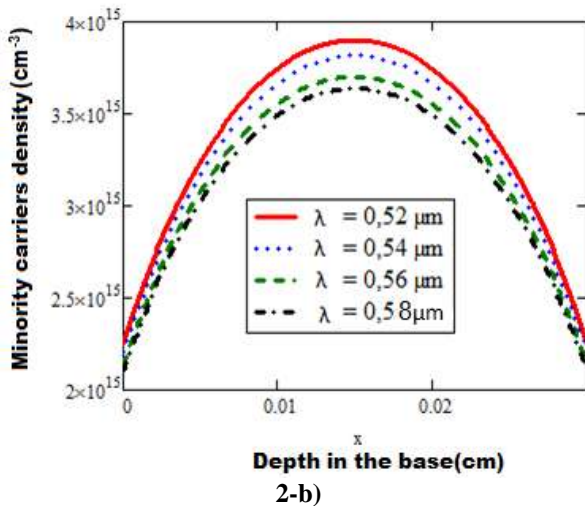


Fig. 2: Variation of the density of minority carriers according to the thickness x of the base.

$Z=0.0001\text{cm}$; $L_0=0.01\text{cm}$; $kl=5\text{cm}^2/\text{s}$; $\phi=50\text{MeV}$;
 $S_f=3.10^3\text{cm/s}$; $H=0.03\text{cm}$

The density of minority carriers according to the thickness x of the base keeps the same profile for different values of the wavelength λ .

The density profile is symmetrical to the axis $x = \frac{H}{2}$ because there are two identical junctions ($x = 0$ and $x = H$) of either side of the considered base.

For $0 < x < \frac{H}{2}$, the gradient of the density of minority carriers in the base is positive and this corresponds to a flow of electrons which go through the base-emitter junction ($x = 0$) thus giving a photocurrent.

For $x = \frac{H}{2}$, the density of minority carriers in the base and maximum gradient is zero. The further away from the junction, the higher the density increases due to a reduction of surface recombination.

The illumination, just like the doping being homogeneous, this area of the base will have a higher carrier density because recombination is less strong there.

For $\frac{H}{2} < x < H$ gradient to load the minority carrier density is always positive because there's another junction between the base and the emitter located at position $x = H$ (fig. 1). There's also at this junction a flow of electrons.

In the junctions ($x = 0$ and $x = H$) the density is minimal because the recombination surface is very strong at these levels.

We also note that the density increases with the wavelength in the interval $[0.40\mu\text{m}; 0.50\mu\text{m}]$ because the carrier generation is very high with sufficiently energetic photons and surface recombinations reduce. We find the inverse effect in

the $[0.52\mu\text{m}; 0.80\mu\text{m}]$, the photogenerated carriers have less and less energy and recombination in volume combined with those surface are reducing the density.

3.2 Photocurrent Density Profile

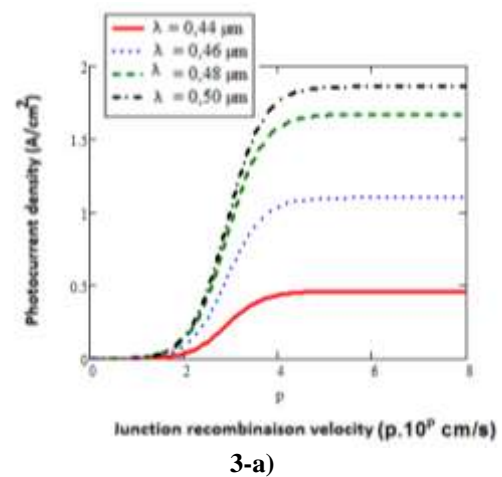
The solar cell's photocurrent obtained from the gradient of the minority carrier density is given by the expression [10]:

$$J_{ph} = 2q \cdot D \cdot \left. \frac{\partial \delta(x, z, S_f, \lambda, kl, \phi)}{\partial x} \right|_{x=0} \quad (10)$$

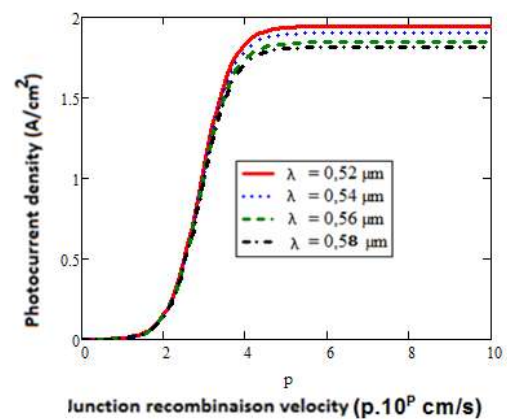
Where q is the elementary charge and D is the diffusion coefficient of electrons in the base. From where:

$$J_{ph} = 2q \frac{S_f L^3 \alpha_i (1-R) F \exp(-\alpha_i z) \tanh\left(\frac{H}{2L}\right)}{S_f L + D \tanh\left(\frac{H}{2L}\right)} \quad (11)$$

Fig. 3a and 3b represent the profile of the photocurrent density according to the recombination velocity at the junction for different values of the wavelength λ



3-a)



3-b)

Fig. 3: Variation of the photocurrent density according to the recombination velocity at the junction S_f ($p.10^9 \text{ cm/s}$) for different values of λ . ($z=0.0001\text{cm}$; $L_0=0.01\text{cm}$; $kl=5\text{cm}^2/\text{s}$; $\phi=50\text{MeV}$; $H=0.03\text{cm}$)

The photocurrent density is zero for low values of the recombination velocity at the junction translating operation of the solar cell in open circuit. The open-circuit's situation corresponds to the blocking of minority charge at the junction.

The density gradually increases to an asymptotic value corresponding to the short-circuit photocurrent when the recombination velocity at the junction becomes larger.

The short-circuit state is a massive transfer of electrons arriving at the junction to the emitter.

When the wavelength increases the density of the photocurrent maintains the same profile and we note an increase of the short-circuit current in the interval $[0.40\mu\text{m}; 0.50\mu\text{m}]$

The increase in wavelength causes a growth in the contribution of the minority carriers of the base in the current supplied by the solar cell because we have a carrier density increases.

In the interval $[0.52\mu\text{m}; 0.80\mu\text{m}]$ is the opposite effect was noted

3.3 Photovoltage Profile

The photovoltage created by the accumulation of minority charge carriers at the junction, is obtained from the relationship of BOLTSMANN [12]:

$$V = V_T \cdot \ln \left[1 + \frac{N_b}{n_0^2} \cdot \delta(0, z, \lambda, kl, \phi, Sf) \right] \quad (12)$$

$V_T = \frac{KT}{e}$ thermal voltage

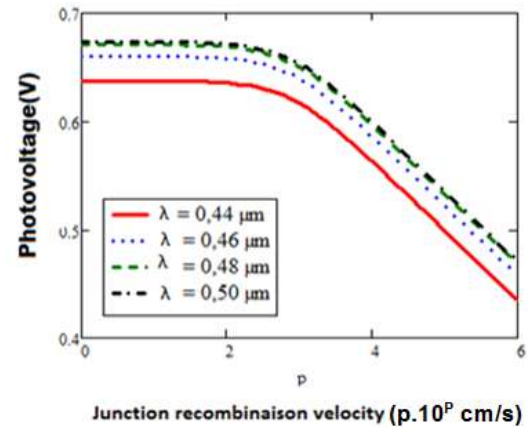
Nb: doping rate of acceptor atoms in the base

n_0 : is the intrinsic carrier density at thermal equilibrium.

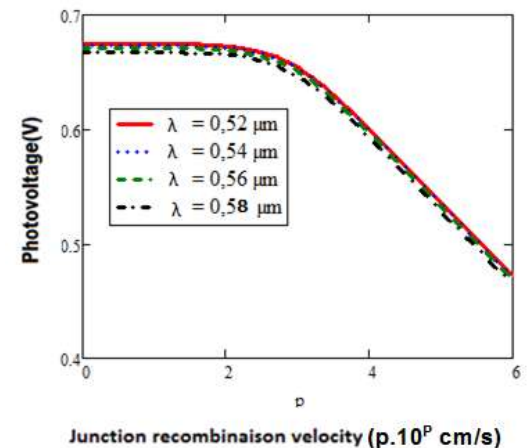
Thus:

$$V_{ph} = \frac{KT}{q} \ln \left\{ 1 + \frac{N_b}{n_0^2} \left[\frac{D \tanh\left(\frac{H}{2L}\right)}{S_f L + D \tanh\left(\frac{H}{2L}\right)} \right] \cdot \frac{L^2}{D} \cdot \alpha_i (1-R) \cdot F \cdot \exp(-\alpha_i \cdot z) \right\} \quad (13)$$

Fig. 4a and 4b show the profile of the photovoltage according to the recombination velocity at the junction S_f ($p.10^p$ cm/s) for different values of the wavelength λ .



4-a)



4-b)

Fig. 4: Variation of the photovoltage according to the recombination velocity at the junction S_f for different values of λ ($z=0.0001\text{cm}$; $kl=5\text{cm}^2/\text{s}$; $\phi=50\text{MeV}$; $L_0=0.01\text{cm}$; $H=0.03\text{cm}$)

Photovoltage decreases with S_f recombination velocity. For large values of S_f , the photovoltage tends towards zero, which corresponds to the solar cell's operation in short-circuit. For low values of S_f , there is no passage of charge at the junction, the photovoltage is constant and its value corresponds to the voltage of open-circuit V_{oc} .

We have further remarks that the photovoltage is even smaller than the wavelength λ is small in the range $[0.40\mu\text{m}; 0.50\mu\text{m}]$.

The increase in wavelength causes a growth in the value of V_{oc} because the amount of stored carriers is greater.

In the interval $[0.52\mu\text{m}; 0.80\mu\text{m}]$ an opposite effect was noticed.

Photovoltage decreases with S_f recombination velocity. For large values of S_f , the photovoltage tends towards zero, which corresponds to the solar cell's operation in open-circuit. For low values of S_f , there is no passage of charge at the junction, the photovoltage is constant and its value corresponds to the open-circuit voltage V_{oc} .

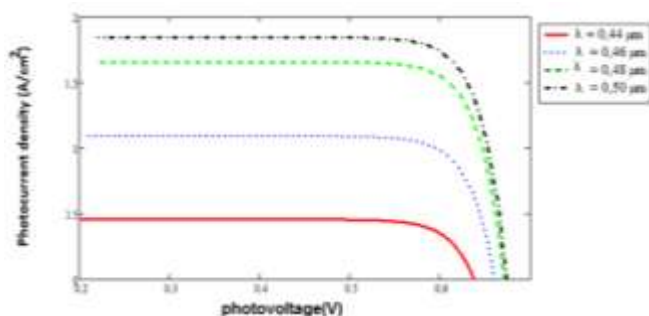
Beyond We notice that the photovoltage is even smaller than the wavelength is small in the range $[0.40\mu\text{m}; 0.50\mu\text{m}]$. The increase in wavelength causes a growth in the value of V_{oc} because the amount of stored carriers is bigger.

In the interval $[0.52\mu\text{m}; 0.80\mu\text{m}]$ is the opposite effect was remarked.

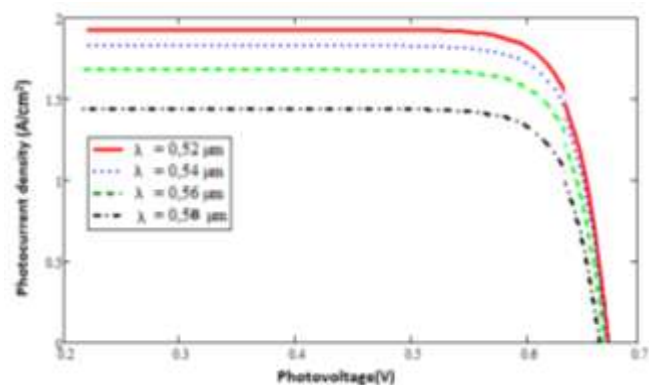
3.4 Electrical Parameters of Solar Cell

3.4.1 Characteristic V-I

The 05-a and 05-b fig. below show the profile of the photo-current density according to the photovoltage



5-a)



5-b)

Fig. 5: V-I characteristic of the solar cell ($z=0.0001\text{cm}$; $L_0=0.01\text{cm}$; $kl=5\text{cm}^2/\text{s}$; $\phi=50\text{MeV}$; $H=0.03\text{cm}$)

The analysis of the characteristic shows that the photovoltage is not independent from the photocurrent [3], [4] added and deduced that the solar cell has two operating modes.

The solar cell behaves as a real voltage generator in the vicinity of the open circuit and as a real current generator in the vicinity of the short circuit.

For each mode of operation, an equivalent electrical circuit to the photocell is proposed.

3.4.2 Shunt Resistance

When the solar cell behaves like a real current generator, the equivalent electrical circuit to the solar cell is as follows: [2]- [5]

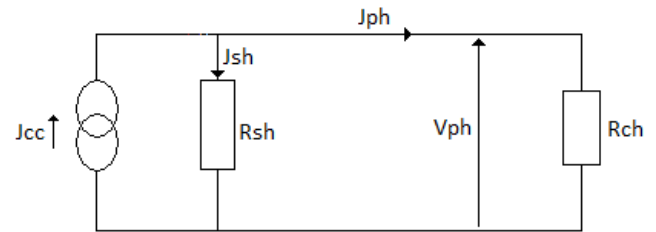


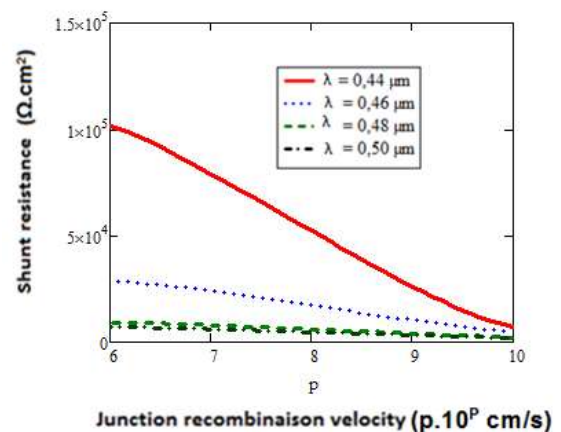
Fig. 6: Equivalent circuit of the solar cell (current generator)

The study of this circuit, allows us to establish the expression of the shunt resistor: [4]-[6]

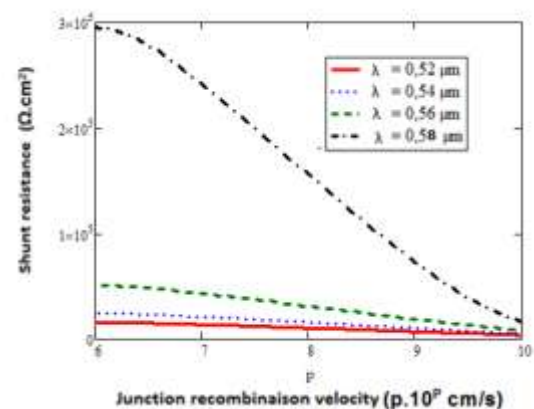
$$R_{SH}(S_f, \lambda, kl, \phi, z) = \frac{V_{PH}(S_f, \lambda, kl, \phi, z)}{J_{CC}(\lambda, kl, \phi, z) - J_{PH}(S_f, \lambda, kl, \phi, z)} \quad (14)$$

J_{cc} represents the short -circuit photocurrent density.

Fig. 7-a and 7-b show the shunt resistance profile according to the recombination velocity at the junction S_f ($\text{p.}10^p \text{ cm s}^{-1}$) for different wavelength values.



7-a)



7-b)

Fig. 7: the shunt resistance variation according to the recombination velocity at the junction for different values of the wavelength λ . ($z = 0.0001\text{cm}$; $L_0 = 0.01\text{cm}$; $kl = 5\text{cm}^2/\text{s}$; $\phi = 50\text{MeV}$; $H = 0.03\text{cm}$)

For different values of the wavelength, there is obtained the shunt resistance profile according to the recombination velocity at the junction in Fig.7. The shunt resistance decreases while keeping the same profile when the wavelength λ increases in the interval $[0.40\mu\text{m}; 0.50\mu\text{m}]$. When the wavelength increases, there is a growth of the short-circuit current

The increase in the short-circuit current is accompanied by the existence of leakage currents. The shunt resistance modeling the parasitic currents; when they increase in value shunt resistance corresponding decrease.

Given the shunt resistance values and photovoltage obtained leakage currents have very little impact on the current supplied by the solar cell.

In the interval $[0.52\mu\text{m}; 0.80\mu\text{m}]$ is the opposite effect was noted.

By giving S_f , recombination velocity at the junction, a value in the vicinity of the short circuit we can draw the following table:

Table 1-a: shunt resistance according to the wavelength λ for $S_f = 7 \times 10^7 \text{ cm/s}$

| $S_f(\text{cm/s})$ | $\lambda(\mu\text{m})$ | $R_{SH}(\Omega.\text{cm}^2)$ |
|--------------------|------------------------|------------------------------|
| 7×10^7 | 0.52 | 0.1×10^5 |
| 7×10^7 | 0.54 | 0.2×10^5 |
| 7×10^7 | 0.56 | 0.5×10^5 |
| 7×10^7 | 0.58 | 2.8×10^5 |

Table 1-b: shunt resistance according to the wavelength λ for $S_f = 7 \times 10^7 \text{ cm/s}$

| $S_f(\text{cm/s})$ | $\lambda(\mu\text{m})$ | $R_{SH}(\Omega.\text{cm}^2)$ |
|--------------------|------------------------|------------------------------|
| 7×10^7 | 0.44 | 0.8×10^5 |
| 7×10^7 | 0.46 | 2.8×10^4 |
| 7×10^7 | 0.48 | 1.2×10^4 |
| 7×10^7 | 0.50 | 1.1×10^4 |

This helps us to trace the graphs $R_{SH} = f(\lambda)$

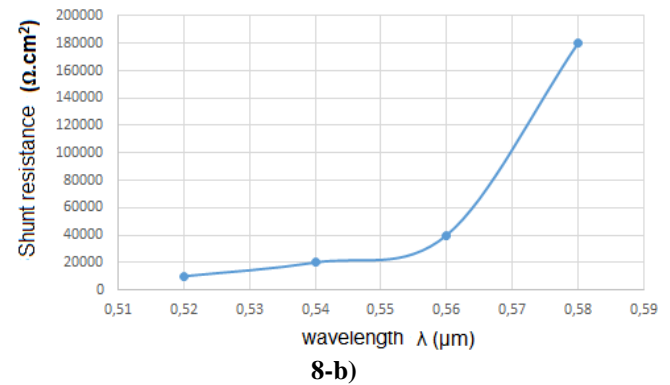
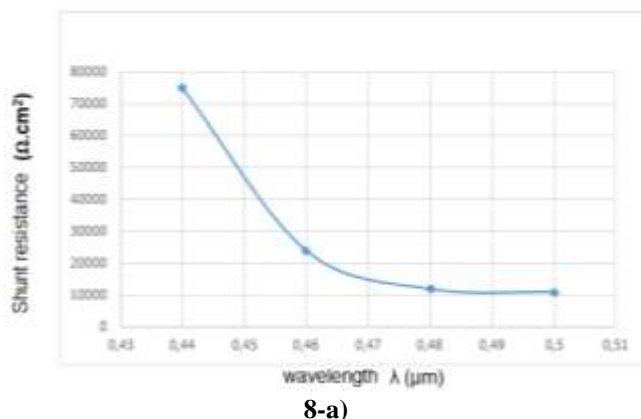


Fig. 8: shunt resistance according to the wavelength ($z = 0.0001\text{cm}$; $L_0 = 0.01\text{cm}$; $kl = 5\text{cm}^2/\text{s}$; $\phi = 50\text{Mev}$; $H = 0.03\text{cm}$)

In the wavelength interval $[0.40\mu\text{m}; 0.50\mu\text{m}]$, the photocurrent density increases with the wavelength; which causes higher leakage currents a decrease in the shunt resistance. In the interval $[0.52\mu\text{m}; 0.80\mu\text{m}]$ the opposite effect is noticed.

3.4.3 Series Resistance

The equivalent circuit model when the solar cell works like a real voltage generator is as follows: [2]-[5]

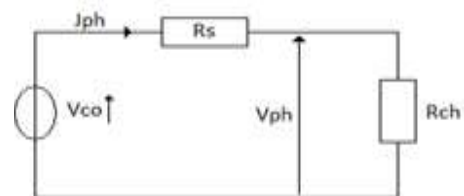
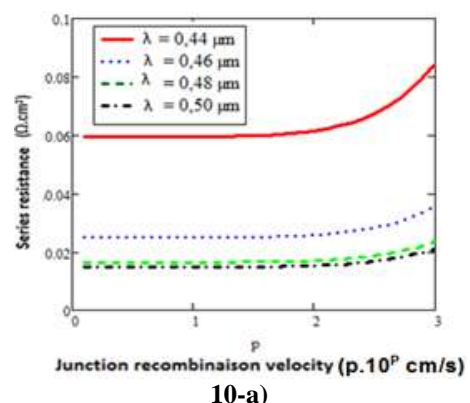


Fig. 9: Equivalent circuit of the solar cell (voltage generator)

From the study of the electrical circuit, the resistance's expression is deduced: [4]-[6]

$$R_s(S_f, \lambda, kl, \phi, z) = \frac{V_{CO}(\lambda, kl, \phi, z) - V_{PH}(S_f, \lambda, kl, \phi, z)}{J_{PH}(S_f, \lambda, kl, \phi, z)} \quad (15)$$

Fig. 10-a and 10-b show the series resistance profile according to the recombination velocity at the junction S_f ($p \cdot 10^p \text{ cm s}^{-1}$) for different wavelength values.



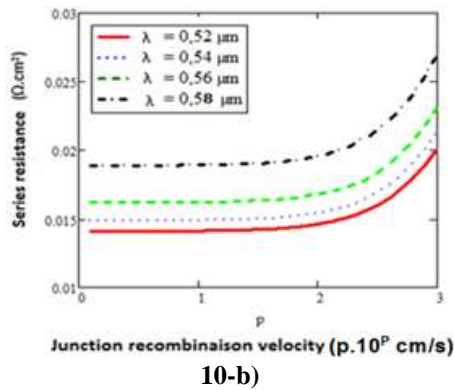


Fig. 10: Variation of the series resistance according to the recombination velocity at the junction for different values of the wavelength λ . ($z = 0.0001\text{cm}$; $L_0 = 0.01\text{cm}$; $k_l = 5\text{cm}^2/\text{s}$; $\phi = 50\text{Mev}$; $H = 0.03\text{cm}$)

For different values of the wavelength, we obtain the series resistance profile according to the recombination velocity at the junction in fig.10.

This profile is the same for different values of the wavelength.

If the wavelength increases the photocurrent density increases in the interval $[0.40\mu\text{m}; 0.50\mu\text{m}]$, which means that the resistive effects of the material thus decreasing the series resistance.

We have the opposite effect in the $[0.52\mu\text{m}; 0.80\mu\text{m}]$.

By giving S_f , recombination velocity at the junction, a value near the open-circuit, we can draw the following table:

Table 2-a: series resistance according to the wavelength λ for $S_f = 10\text{ cm/s}$

| $S_f(\text{cm/s})$ | $\lambda(\mu\text{m})$ | $R_s(\Omega\text{cm}^2)$ |
|--------------------|------------------------|--------------------------|
| 10 | 0.44 | 0.06 |
| 10 | 0.46 | 0.024 |
| 10 | 0.48 | 0.018 |
| 10 | 0.50 | 0.016 |

Table 2-b: series resistance according to the wavelength λ for $S_f = 10\text{ cm/s}$

| $S_f(\text{cm/s})$ | $\lambda(\mu\text{m})$ | $R_{SH}(\Omega\text{cm}^2)$ |
|--------------------|------------------------|-----------------------------|
| 10 | 0.52 | 0.013 |
| 10 | 0.54 | 0.015 |
| 10 | 0.56 | 0.016 |
| 10 | 0.58 | 0.018 |

This allows us to draw graphs $R_s = f(\lambda)$

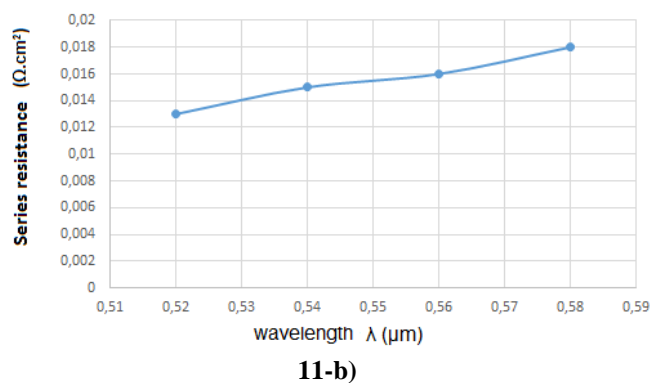
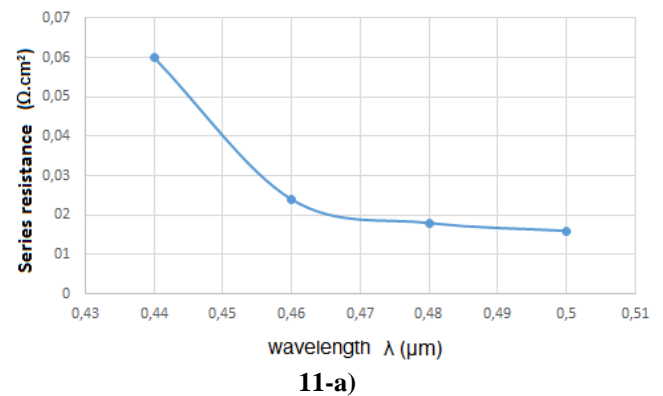


Fig. 11: Series resistance according to the wavelength λ to $S_f = 10\text{ cm/s}$ ($z = 0.0001\text{cm}$; $L_0 = 0.01\text{cm}$; $k_l = 5\text{cm}^2/\text{s}$; $\phi = 50\text{Mev}$; $H = 0.03\text{cm}$)

In the wavelength interval $[0.40\mu\text{m}; 0.50\mu\text{m}]$, the series resistance decrease with wavelength since the photocurrent density increases; that is to say the conduction losses decrease because the resistivity of the material decreases. We have the inverse effect in the interval $[0.52\mu\text{m}; 0.80\mu\text{m}]$.

4. CONCLUSION

The resolution of the continuity equation allowed us to establish the expression of minority carrier density of excess charge in the base of the solar cell.

From this density, the terms of the photocurrent density and photovoltage according to the wavelength has been deducted. From equivalent electrical models, expressions of series and shunt resistors have been established.

The influence on all electrical quantities was studied. The study was done in the visible range.

We noted that in the interval $[0.40\mu\text{m}; 0.50\mu\text{m}]$, the electrons density in the base increases with the wavelength because the generation of minority carriers in the base dominates recombination, which resulted in the growth of short-circuit current and the open-circuit photovoltage and a decrease of the electrical parameters of the solar cell.

In the interval $[0.52\mu\text{m}; 0.80\mu\text{m}]$, we noticed inverse effects

REFERENCES

- [1]. Kraner, H.W. (1983) radiation damage in silicon detectors, 2nd Pisa meeting on Advanced Detectors, Grosseto, Italy, June 1983, 3-7.
- [2]. Mbodj, S., Ly, I., Diallo, H.L., Dione, M.M., Diassé, O., Sissoko, G. (2012) Modeling study of N⁺/P Solar Cell Resistances from Single I-V characteristics curve considering the Junction recombination velocity, Research Journal of Applied sciences, Maxwell scientific organization, **4(1)**, 1-7.
- [3]. Sissoko, G., Nanema, E., Correa, A., Biteye, P.M., Adj, A., Ndiaye, A.L. (1998) silicon solar cell recombination parameters determination using the illuminated I-V characteristic, Renewable energy, Elsevier science Ltd, **3**, 1848-1851.
- [4]. Samb, M.L., Zoungrana, M., Toure, F., Diop, M.T.D., Sissoko, G. (2010) Etude en modélisation à 3-D d'une photopile au silicium en régime statique placée dans un champ magnétique et sous éclairage multispectral, journal des sciences, **10**, 23-38.
- [5]. Dione, M.M., Mbodj, S., Samb, M.L., Dieng, M., Thiam, M., Ndiaye, S., Barro, F.I., Sissoko, G. (2009) Vertical Junction Under constant Multispectral Light : Determination of recombination parameters, 24th European photovoltaic solar energy conference and exhibition, Germany, 2009, 465-469.
- [6]. Diallo, H.L., Dieng, B., Ly, I., Dione, M.M., Ndiaye, M., Lemrabott, O. H., Bako, Z.N., Wareme, A., Sissoko, G. (2012), Determination of the recombination and electrical parameters of a vertical multijunction silicon solar cell, Research Journal of Applied sciences, Maxwell scientific organization, 2012, **4(16)**, 2626-2631.
- [7]. Diao, A., Wade, M., Zoungrana, M., Sarr, M., Ndiaye, M., Thiam, N., Thiam, A., Dieng, A., Ngom, M., Maiga, A.S., Sissoko, G. (2011) modèles électriques équivalents en régime dynamique fréquentiel de l'impédance d'une photopile bifaciale sous l'effet d'un champ magnétique constant pour un éclairage polychromatique par la face arrière, journal des sciences, **11**, 20-26.
- [8]. Dione, M.M., Diallo, H.L., Wade, M., Ly, I., Thiam, M., Toure, F., Gueye, A.C., Dieme, N., Bako, Z. N., Mbodj, S., Barro, F.I., Sissoko, G. (2011) Determination of the shunt and series resistances of a vertical multijunction solar cell under constant multispectral light Proceedings of the 26th European Photovoltaic Solar Energy Conference, 2011, 250 - 254.
- [9]. Samb, M.L., Zoungrana, M., Toure, F., Diop, M.T.D., Sissoko, G. (2010), Etude en modélisation à 3-D d'une photopile au silicium en régime statique placée dans un champ magnétique et sous éclairage multispectral, journal des sciences, **10**, N°4, 23-38.
- [10]. Arora, J.D., Singh, S.N., Mathur, P.C. (1981) surface recombination effects on the performance of N⁺p step and diffused junction silicon solar cell, Solid state electronics, **24(8)**, 739-749.
- [11]. Bouzidi, K., chegaar, K., Bouhemadou, A. (2007) Solar cells parameters evaluation considering the series and shunt resistance. Solar Energ. Mater. Solar cells, **91**, 1647-1651.
- [12]. Bashahu, M. and Habyarimana A., (1995) Review and test of methods for determination of the solar cell series resistance. Renew Energy, **6(2)**, 127-138.
- [13]. El-Adawi, M.K and Al-Nuaim, I.A. (2002) A method to determine the solar cell series resistance from single I-V characteristic curve considering to shunt resistance. New approach. Vacuum, **64**, 33-36.
- [14]. Sissoko, G., Museruka, C., Correa, A., Gaye, I., Ndiaye, A.L. (1996) Light spectral effect on recombination parameters of silicon solar cell. World renewable energy congress, part III, 1996, 1487-1490.
- [15]. Wise, J.F., (1970) Vertical junction hardered solar cell. U.S. Patent No. 3690853
- [16]. Dieng, A., Sow, M.L., Mbodj, S., Samb, M.L., Ndiaye, M., Thiame, M., Barro, F.I., Sissoko, G. (2009) 3D study of a polycrystalline silicon solar cell: influence of an applied magnetic field on the electrical parameters, proceeding of the 24th European photovoltaic solar energy conference, 2009, 473-474.
- [17]. Mandougou, S., Made, F., Boukary, M.S., Sissoko, G. (2007) I-V characteristic for bifacial silicon solar cell studied under a magnetic field, Advanced Materials Research, **18-19**, 303-312.
- [18]. Boer, K.W. (2010) Introduction to space charge effects in semiconductors. Springer-Verlag
- [19]. Moller, H.J., (1993) semiconductors for solar cell, Artechhouse.
- [20]. Orton, J.W and Blood, P. (1990) The electrical characterization of semiconductor: Measurement of minority carrier properties. Academic press, London.
- [21]. Misiakos, K., Wang, C.H., Neugrochol, A., Lindholm, F.A. (1990) Simultaneous extraction of minority carrier parameters in crystalline semiconductors by lateral photocurrent. J. App. Phys., **67(2)**, 767-772.
- [22]. Dugas, J. (1994) Solar energy materials and solar cells, **32**, 71-88.
- [23]. Barro, F.I., Mbodj, S., Ndiaye, M., Maiga, A.S., Sissoko, G. (2008) Bulk and surface recombination parameters of silicon solar cell under constant white bias light. J. SCI, **8(4)**, 37-41.